Uncertainty Modelling in Linear Dynamic Systems: A Feedback Point of View

Technical Report by Dr Paresh Date,
Centre for Analysis of Risk and Optimisation Modelling Applications (CARISMA), Brunel University, UK.

Abstract

This report is written with two purposes in mind. First, it brings together some recent results in the area of closed-loop model validation for dynamic feedback systems. The central idea of the methods presented here is to map uncertainty given in a physically meaningful domain into an uncertainty description which is useful from a robust control design and analysis point of view. Secondly, this report also presents a brief but self-contained glimpse of control theoretic tools to mathematicians unfamiliar with this field. It is hoped that the expositions such as this one will open new collaborations between other branches of mathematics (in particular, operations research which deals with large scale static uncertainty modelling) and control theory.

Contents

List of Figures

Chapter 1

Preliminaries

Here, we introduce the subject to be addressed in this report. The discussion in this chapter is somewhat heuristic and is aimed for non-specialist audience. The further chapters will require some background in functional analysis and complex analysis or in control theory. However, an effort is made throughout the report to keep the discussion as self-contained as possible.

Feedback based control is used in a large number of engineering and biomedical systems; only a few examples are provided here. An aircraft altitude is measured (or 'fed back') by altitude sensors and an algorithm (implemented through hardware and/or software) uses this information to compute appropriate input to move control surfaces on wings (actuators) to correct any deviation from the desired altitude. In a modern automobile engine, the measurements from exhaust gas emission sensors is used to adjust the air-to-fuel ratio in the combustion chamber. Human body contains several complex feedback loops; increase in blood sugar, for example, will trigger a sequence of chemical actions which will conteract this increase. Recently, field trials are underway for use of automatic feedback control for drug administration in anaesthetized surgical patients. In such cases, the use of feedback (as measured by the patient's response to the drug infusion) may help the physicians to avoid underdosage or overdosage. Any application where the input of a dynamic system is affected by its measured output may be analysed (and where possible, designed) using the feedback framework.

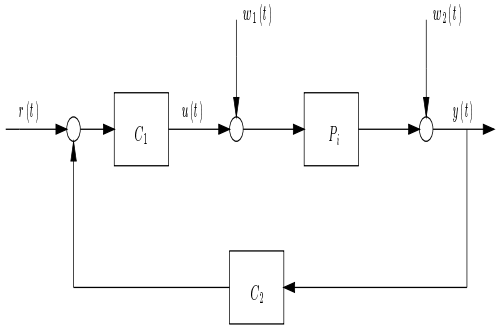

Figure 1.1: Closed Loop System

Feedback controllers are designed using a mathematical model of the system and are implemented in software and/or hardware. Fig 1.1 shows a feedback loop schematically. In this figure, C_1 and C_2 are *feedforward* and *feedback* components of controller $C = C_1 \times C_2$. C_1, C_2 and P are dynamic systems and $r(t)$, $w_1(t)$ and $w_2(t)$ are signals affecting them. $u(t)$ and $y(t)$ represents the input and the output of the system respectively. The systems may be multivariable, *i.e.* the signals involved may be vector valued. The closed loop transfer functions (or Laplace transforms of the underlying differential operators) are given by

$$\begin{aligned} T_{r\mapsto u} &= (I - CP)^{-1}C_1, \quad T_{r\mapsto y} &= P(I - CP)^{-1}C_1 \\ T_{w_1\mapsto u} &= (I - CP)^{-1}CP, \quad T_{w_1\mapsto y} &= (I - CP)^{-1}P \\ T_{w_2\mapsto u} &= (I - CP)^{-1}C, \quad T_{w_2\mapsto y} &= (I - CP)^{-1} \end{aligned}$$

where $T_{x\mapsto z}$ is a transfer function from signal $x(t)$ to signal $z(t)$ and I represents an identity operator of appropriate dimensions.

Controller C is often (though not always) designed from specifications about frequency response of these transfer functions (*e.g.*) one may want $T_{r\mapsto y}(j\omega)$ to be large at low frequencies $0 \leq \omega \leq \omega_l$ and $T_{w_2\mapsto y}$ to be small at high frequencies (so that the response of $y(t)$ to high frequency sensor noise is attenuated, but its tracking performance with respect to reference level changes at $r(t)$ is unaffected.) To see the role of feedback, note the following:

- The only way the transfer functions $T_{w_1\mapsto y}$ and $T_{w_2\mapsto y}$ (*i.e.* in most physical systems, the effects of sensor and actuator noise on the output) can be manipulated (and hence the noise may be attenuated) is via feedback.

- Even if P itself is unstable, all the above transfer functions mapping external signals r, w_1, w_2 to u and y can be made stable.

It is worth adding that the closed loop may have unstable operators (i.e. the output may grow unbounded for a bounded input)[1], irrespective of whether the open loop system P is stable. It is the responsibility of control designer to ensure that the designed loop is stable and achieves the desired performance. The issues in stability and robustness in control design are beyond the scope of this report; the reader is referred to [ZDG96].

For the purpose of this report, all the systems involved are assumed to be linear and time invariant. This assumption is often valid in practice as the range of behaviour of the system under study is often linear. Even when this is not the case, it is often useful to design a linear controller first and then introduce nonlinear elements to analyse their impact.

To design a controller, a model of the system to be controlled is needed. A parameterized model of the true system is identified either from physical knowledge about the system and/or from measured input-output experimental data. Inevitably, there is a discrepancy between the true

[1] An example of an unstable operator is $\frac{1}{s-1}$, whose impulse response grows exponentially with time. Any forced differential equation (*i.e.* one with a forcing function) whose solution has exponentially increasing terms is unstable.

system and its model. This discrepancy introduces a corresponding discrepancy in the designed closed loop (*i.e.* the one with the model and controller) and the achieved closed loop (i.e. one with the true system and the implemented controller). There is a risk that the designed closed loop is stable and yields the desired performance, but the achieved closed loop performs poorly and may even be unstable. In an industrial control environment, this has an implication on the profitability of business. As an example, Lack of good models and hence of good controllers for unstable gas fired combustors forces power generation companies to operate power plants at a lower than maximum efficiency [Dow01]. Hence is necessary to quantify the uncertainty in identification from a closed loop point of view and validate whether the designed controller will perform adequately when in closed loop with the true system.

The results presented in this technical report are centered around a relationship of the form

(closed-loop performance of [true system, controller]) $\geq$ (closed-loop performance of [model, controller]) - distance(true system, model).

The second term does *not* include the control algorithm *i.e.* the relationship is valid for any controller (which stabilises both the true system and the model). The remainder of the report is structured as follows. Chapter 2 outlines some mathematical preliminaries and basic results related to closed loop behaviour of linear systems. It introduces the notion of distance between systems and of the closed loop performance for which the relationship mentioned above holds true. Chapter 3 is based on the author's work with Dr M. Cantoni and presents two different results on validation of closed loop validation and demonstrates it with simulation example. Chapter 4 briefly outlines some of the related work by Dr X. Bombois and his co-workers (including the author). Finally, chapter 5 shows how to yield information about behaviour over a continuum of frequencies based on data for a finite frequencies and knowledge of complexity of the involved systems.

Chapter 2

The $\nu-$gap Metric

2.1 Notation

Let $\mathbb{D} := \{z \in \mathbb{C} : |z| < 1\}$ and $\partial\mathbb{D}$ denote the boundary of $\mathbb{D}$. The symbol $\mathcal{L}_\infty$ is used to denote the space of all (possibly matrix valued) functions $F(z)$ that are essentially bounded on $\partial\mathbb{D}$ and have finite norm $\|F\|_{\mathcal{L}_\infty} := \text{ess sup}_\omega \overline{\sigma}(F(e^{j\omega}))$, where $\overline{\sigma}(\cdot)$ represents the maximum singular value. The symbol $\mathcal{H}_\infty$ denotes the space of functions $F(z)$ that are analytic in $\mathbb{D}$ and have finite norm $\|F\|_\infty := \sup_{z\in\mathbb{D}} |f(z)| < \infty$. Systems whose z transfer functions are in $\mathcal{H}_\infty$ are *stable i.e.* a bounded input always produces a bounded output [1]. Given a system transfer function $F(z)$, the transfer function of the adjoint system is denoted by $F^*(z) := F(\frac{1}{z})^T$, where the superscript 'T' denotes matrix transpose. Note that for a real rational transfer function $F^*(e^{j\omega}) = \overline{F(e^{j\omega})}^T$, where the overline denotes complex conjugate.

Any linear, time invariant discrete-time system P that is stabilisable, can be expressed as $P = NM^{-1} = \tilde{M}^{-1}\tilde{N}$ with

1. $G_P := \begin{bmatrix} N \\ M \end{bmatrix}$ inner (*i.e.* $G_P^* G_P = I$) and left invertible in $\mathcal{H}_\infty$; and
2. $\tilde{G}_P := \begin{bmatrix} -\tilde{M} & \tilde{N} \end{bmatrix}$ co-inner (*i.e.* $\tilde{G}_P \tilde{G}_P^* = I$) and right invertible in $\mathcal{H}_\infty$.

G_P (resp. $\tilde{G}_P$) is called the normalised right (resp. normalised left) graph symbol of plant P [2].

Note, any $X = G_P Q$ for $Q, Q^{-1}\mathcal{H}_\infty$ is also left invertible in $\mathcal{H}_\infty$ and is also a *right coprime factorisation* for P. Similar statement holds for $\tilde{X} = \tilde{Q}\tilde{G}_P$, $\tilde{Q}, \tilde{Q}^{-1} \in \mathcal{H}_\infty$.

2.2 Introduction

Feedback can reduce the sensitivity of a designed system to uncertainty arising, for example, from the inevitable mismatch between open-loop models used in the design process and the physical sys-

[1] This is not the only definition of stability; but will suffice for the purpose of this report.

[2] As is the convention in control theory, the true system is often referred to as *plant* in this report.

tems that these models represent. Indeed, significant research has been dedicated to understanding, both quantitatively and qualitatively, the uncertainty that the feedback mechanism can handle. For general linear systems, gap-like metrics are known to capture the difference between open-loop systems from the perspective of their behaviour in closed-loop [Vid85, GS90, Vin01, CV02]. The focus of section 2.4- and indeed, of the remainder of this report - is the robustness results related to the ν-gap metric. Before introducing $\nu-$gap metric, the topic of so called $\mathcal{H}_\infty$ control is briefly introduced.

2.3 Interlude 1: $\mathcal{H}_\infty$ Control

$\mathcal{H}_\infty$ control (so called as it usually involves minimisation of ∞-norm of a closed loop transfer matrix) has now gained a wide acceptance in automobile and aeronautical industries as a control design paradigm of choice. There is a huge body of literature on theory and application of robust control; see [PG99], [XFS01], [FG] for examples of a few applications. Here, only a specific, simple example of an objective function for $\mathcal{H}_\infty$ control design is considered and its implications are reviewed. Consider the system in figure 1.1. Suppose, for a given single input, single output P_i, a controller C is found such that

1. All the transfer functions in figure 1.1 are stable and
2. $\left\|\alpha(I-CP)^{-1}C\right\|_\infty \leq \epsilon$ for a given $\epsilon > 0$ and for a user chosen scalar transfer function $\alpha \in \mathcal{H}_\infty$.

Then the following facts hold:

1. (*Robust Stability Interpretation.*) The controller C stabilizes all the plants from an uncertain plant set defined by
$$\Pi = \{P : P = P_i + \alpha\Delta, \Delta \in \mathcal{H}_\infty, \|\Delta\|_\infty \leq \epsilon^{-1}\}$$
2. (*Nominal Performance Interpretation.*) Given any w_2 in figure 1.1 with spectrum $|\alpha(e^{j\omega})|^2$, the input u ot P_i due to w_2 will have a spectrum bounded by ϵ^2 [3].

Note that, unlike the notion of uncertainty in most other fields of mathematics, no statistical assumptions are made about Δ and no assumptions are made about the distribution of w_2 (spectrum is only a second order property). These uncertainty descriptions are often referred to as *deterministic* uncertainty descriptions.

Various descriptions of uncertainty (other than the additive uncertainty above) are possible and most can be analysed using Linear Fractional Transformation (LFT) framework ([ZDG96], chapter). Depending on the uncertainty description and performance requirements, various control

[3] $\mathcal{H}_\infty$ control is often motivated by amplification of square summable signals which lead to nicer theoretical interpretation. We will not discuss it here; the reader is referred to [ZDG96].

design problems may be posed as $\mathcal{H}_\infty$ norm minimisation problems. There are efficient numerical procedures available to solve problems such as the one above using solution of a pair of algebraic Riccati equations. These procedures are already available in commercial software such as MATLAB. Importantly, the above framework and interpretations and procedures are valid for multivariable systems.

The criterion of performance and the uncertainty description used in this report is somewhat more sophisticated than the additive uncertainty desciption above. It relies on the idea of measuring distance between systems in terms of the size of perturbations in normalized coprime factors.

2.4 Review of $\nu-$gap metric robustness results

The notion of measuring distance between linear systems in terms of distance between their graph spaces was introduced by Vidyasagar in [Vid84]. In this paper, a metric called the graph metric was introduced which is characterised by the smallest distance, in a certain sense, between the coprime factors of two systems. This work was followed by a number of advances in characterisation and computation of similar metrics under which feedback stability is a robust property. The gap metric [ES85] and the chordal metric [Par92] induce the same topology as the graph metric. In [Vin93a], a metric called the $\nu-$gap metric was defined. It is closely related to the gap metric but has a nicer frequency response interpretation and leads to less conservative robustness results in general.

The $\nu-$gap between two linear time-invariant plants P_1 and P_2 is defined as

$$\delta_\nu(P_1,P_2) = \begin{cases} \inf_{Q,Q^{-1}\in\mathcal{L}_\infty} \| G_{P_1} - G_{P_2}Q \|_\infty & \text{if} \quad I(P_1,P_2)=0 \\ 1 & \text{otherwise} \end{cases}, \tag{2.1}$$

where $I(P_1,P_2) :=$ wno $\det(G_{P_2}^* G_{P_1})$ and wno (g) denotes the winding number of $g(z)$ evaluated on the standard Nyquist contour indented around any poles and zeros on $\partial\mathbb{D}$ [Vin93a]. For a real rational transfer matrix X satisfying $X, X^{-1} \in \mathcal{L}_\infty$ the winding number wno $\det(X) = \eta(X^{-1}) - \eta(X)$ where $\eta(x)$ denotes the number of unstable poles of x. When the winding number condition is satisfied, $\delta_\nu(P_1,P_2)$ equals the $\mathcal{L}_2$ *-gap*:

$$\delta_{\mathcal{L}_2}(P_1,P_2) := \|\tilde{G}_{P_2} G_{P_1}\|_\infty = \sup_\omega \kappa(P_1,P_2)(e^{j\omega}), \tag{2.2}$$

where $\kappa(P_1,P_2)(e^{j\omega})$ is the pointwise *chordal* distance between the stereographic projections of the frequency responses of P_1 and P_2 onto the Riemann sphere, as defined by

$$\kappa(P_1,P_2)(e^{j\omega}) := \overline{\sigma}\left((I+P_2P_2^*)^{-\frac{1}{2}}(P_1-P_2)(I+P_1^*P_1)^{-\frac{1}{2}} \right)(e^{j\omega}). \tag{2.3}$$

Note that, $\kappa(\cdot,\cdot)$ can be computed from purely frequency response data.

Given a controller C and a (possibly frequency weighted) plant P_i, a useful measure of closed-loop performance, which is central to the $\mathcal{H}_\infty$ loop-shaping paradigm for design, is

$$b(P_i,C) = \begin{cases} \|H(P_i,C)\|_\infty^{-1} = \inf_\omega \rho(P_i,C)(e^{j\omega}) & \text{if } C \text{ stabilises } P \\ 0 & \text{otherwise} \end{cases}, \tag{2.4}$$

where

$$\rho(P_i, C)(e^{j\omega}) := \underline{\sigma}(H(P_i, C))(e^{j\omega}),$$

$\underline{\sigma}(\cdot)$ denotes the minimum singular value and the closed-loop transfer function $H(P_i, C)$ is defined by

$$H(P_i, C) := \begin{bmatrix} P_i \\ I \end{bmatrix} (I - CP_i)^{-1} \begin{bmatrix} -C & I \end{bmatrix}$$

This is a transfer function from $\begin{bmatrix} r \\ -w_2 \end{bmatrix}$ to $\begin{bmatrix} u \\ y \end{bmatrix}$ in figure 1.1, with $C_1 = I$. It is known that any controller that stabilises a plant P_1 and achieves $b(P_1, C) > \beta$, also stabilises all plants in the set $\{P_2 : \delta_\nu(P_1, P_2) \leq \beta\}$ [Vin93a]. Further, this measure of performance may also be linked to more conventional measures of control design performance. For a single input, single output system, $b(P, C) > 0.3$ implies a gain margin of at least 1.85 and a phase margin of at least 34.9° [Vin01]. The difference between the level of closed-loop performance achieved by a feedback compensator C with a nominal plant P_1 and with a perturbed plant P_2 can be quantified in terms of $\delta_\nu(P_1, P_2)$ as follows:

$$b(P_2, C) \geq b(P_1, C) - \delta_\nu(P_1, P_2). \tag{2.5}$$

A pointwise-in-frequency version of this performance bound also holds:

$$\rho(P_2, C)(e^{j\omega}) \geq \rho(P_1, C)(e^{j\omega}) - \kappa(P_1, P_2)(e^{j\omega}). \tag{2.6}$$

Indeed (2.5) follows from this since

$$\inf_\omega \Big(\rho(P_1, C)(e^{j\omega}) - \kappa(P_1, P_2)(e^{j\omega})\Big) \geq \inf_\omega \rho(P_1, C)(e^{j\omega}) - \sup_\omega \kappa(P_1, P_2)(e^{j\omega}).$$

These are the relationships alluded to earlier in chapter 1. Note, however, that the pointwise bound in (2.6) is useful only if C is known to stabilise both P_1 and P_2. To this end the following result is easily inferred from the development in [Vin93a] (see also [Vin93b]):

Lemma 1 *Suppose, a true plant P_t, a model P_m and a nominal controller C_n satisfy the following conditions:*

1. *$H(P_t, C_n)$ and $H(P_m, C_n)$ are stable;*
2. *$\kappa(P_t, P_m)(e^{j\omega}) < \rho(P_m, C_n)(e^{j\omega}) \; \forall \, \omega$.*

Then any *other controller C which stabilises P_m and satisfies $\kappa(P_t, P_m)(e^{j\omega}) < \rho(P_m, C)(e^{j\omega}) \; \forall \, \omega$ is guaranteed to stabilise P_t with closed-loop performance*

$$b(P_t, C) \geq \inf_\omega \Big(\rho(P_m, C)(e^{j\omega}) - \kappa(P_m, P_t)(e^{j\omega})\Big). \tag{2.7}$$

Note that the lower bound in (2.7) is tighter than that in (2.5). However, no computationally tractable characterisation for this is known. We will return to (2.7) in chapter 5.

As the true plant is unknown, it is not possible to know $\kappa(P_m, P_t)(e^{j\omega})$ exactly. Depending on the *a priori* information available about the set to which the true plant belongs and possibly, the *a posteriori* measurement data, two different approaches may be taken to estimate $\kappa(P_m, P_t)(e^{j\omega})$:

- Find a system, say $\hat{P}$ which is consistent with the *a priori* information, *a posteriori* data and which *minimises* $\kappa(P_m, P)(e^{j\omega})$ over all systems P which are consistent with the data and the information. Then $\kappa(P_m, \hat{P})(e^{j\omega})$ is the *lower* bound on $\kappa(P_m, P_t)(e^{j\omega})$ and $\rho(P_m, C)(e^{j\omega}) - \kappa(P_m, \hat{P})(e^{j\omega})$ is the best case lower bound on $\rho(P_t, C)$ one may have on true pointwise closed loop performance from the given information. If *even* this best bound is seen as unsatisfactory, then the model-controller loop is said to be invalidated and either the controller needs to be re-designed or a new model needs to be identified. This method was presented in [DC03b] and is discussed in the next chapter.

- Find the worst case pointwise chordal distance $\kappa(P_m, P)(e^{j\omega})$ over all P consistent with the given information. This, in turn, gives the worst lower bound one may have on true pointwise closed loop performance from the given information. If *even* this worst case bound is deemed acceptable, then the controller-model pair may be said to be validated. This approach was presented in [BD03] and is discussed in chapter 4.

Finally, chapter 5 discusses a way of obtaining a bound on $b(P_t, C)$ using pointwise frequency response measurements and an appropriate notion of complexity. This work was first published in [DC03a].

Chapter 3

Pointwise Chordal distance from Closed-Loop Frequency Response Measurements

3.1 Introduction

Most of the results of this chapter were first published in [DC03b].

For the sake of notational simplicity, the single input single output (SISO) case is discussed here. The multiple input multiple output (MIMO) case follows similarly with appropriate notational modifications.

For the problem introduced above the *a priori* information is a model P_m of an unknown true system P_t, and a controller C which stabilises both P_m and P_t. Since it is assumed that C stabilises P_t, frequency response samples of

$$X_t = \begin{bmatrix} I \\ P_t \end{bmatrix} (I - CP_t)^{-1}$$

can be measured at any frequencies of interest. Techniques for achieving this are discussed in [vdHS95, FL98]. Note that, unless C is itself stable, X_t is not necessarily a coprime factorisation of P_t over $\mathcal{H}_\infty$. However, at any frequency ω_i that does not correspond to a pole of C on the unit circle, X_t is left-invertible by $\begin{bmatrix} I & -C(e^{j\omega_i}) \end{bmatrix}$ and hence, the range of $X_t(e^{j\omega_i})$ is the graph of $P_t(e^{j\omega_i})$. Correspondingly, at any such frequency ω_i, the chordal distance

$$\kappa(P_m(e^{j\omega_i}), P_t(e^{j\omega_i})) = \inf_{Q \in \mathbb{C}} \bar{\sigma}(G_m(e^{j\omega_i}) - X_t(e^{j\omega_i})Q), \tag{3.1}$$

where $G_m(e^{j\omega_i})$ denotes the value of any *normalised* right graph symbol for P_m at the frequency ω_i. Such a graph symbol can be constructed from any normalised right coprime factorisation $P_m = N_m D_m^{-1}$ as follows: $G_m = \begin{bmatrix} D_m \\ N_m \end{bmatrix}$. See [Vin01] for further details.

Now, the *a posteriori* information is a vector of (not necessarily uniformly spaced) noisy frequency response samples

$$\overline{X} = \begin{bmatrix} X_1 \; X_2 \; \ldots \; X_n \end{bmatrix}^T,$$

where $X_i = X_t(e^{j\omega_i}) + v_i$, $\omega_i \in [0, \pi)$ and $\|v_i\| \leq \epsilon$ for $i = 1, 2, \ldots, n$ and some specified ϵ. Note that the measured data is to be explained in terms of two components – noise v_i and true system behaviour X_t. The value ϵ bounds the level of data one is prepared to attribute to noise. Since parameters $\rho > 1$ and $\gamma > 0$ such that $X_t \in \overline{B}\mathcal{H}_{\infty,\rho}(\gamma)$ can be determined from additional measured data,[1] it is also sensible to constrain the partitioning of data into noise and true system behaviour in these terms.

In light of this, and bearing in mind the objective of estimating $\kappa(P_m(e^{j\omega_i}), P_t(e^{j\omega_i}))$, consider the following constrained optimisation problem:

$$\min_{\hat{X}_t} \max_i \left(\inf_{Q_i \in \mathbb{C}} \overline{\sigma}(G_m(e^{j\omega_i}) - \hat{X}_t(e^{j\omega_i})Q_i) \right) = \min_{\hat{X}_t} \max_i \kappa(P_m(e^{j\omega_i}), \mathrm{Quot}(\hat{X}_t(e^{j\omega_i}))) \tag{3.2}$$

subject to

$$\hat{X}_t(e^{j\omega_i}) = X_i - v_i, \quad \hat{X}_t \in \overline{B}\mathcal{H}_{\infty,\rho}(\gamma) \quad \text{and} \quad \|v_i\| \leq \epsilon, \tag{3.3}$$

where $\mathrm{Quot}(\begin{bmatrix} X_D \\ X_N \end{bmatrix}) := X_D X_N^{-1}$ and v_i are the decision variables in the optimisation. The purpose and the result of this optimisation may be explained as follows. Let λ be the minimum achieved by solving the above problem (assuming it exists and is unique). Then there exists a system $\hat{X}_t \in \overline{B}\mathcal{H}_{\infty,\rho}(\gamma)$ and bounded noise terms v_i defined pointwise in frequency with $\|v_i\| \leq \epsilon$, $i = 1, 2, \ldots, n$ such that the measured data can be interpolated as

$$X_i = \hat{X}_t(e^{j\omega_i}) + v_i$$

and

$$\max_i \kappa(P_m(e^{j\omega_i}), \mathrm{Quot}(\hat{X}_t(e^{j\omega_i}))) \leq \lambda$$

holds. Put another way, there is no system consistent with the *a priori* assumptions (in terms of ϵ, γ, ρ) and with the *a posteriori* data (in terms of $\overline{X}$) whose worst case chordal distance over $\{\omega_i\}$ is *better* than λ.

3.2 Interlude 2: Linear Matrix Inequalities

Computational algorithms suggested in this report rely heavily on convex optimisation problems subject to Linear Matrix Inequality (LMI) constraints. LMI constraints have the form

$$F(x) = F_0 + \sum_{i=1}^{m} x_i F_i > 0 \; (\text{or } \geq 0) \tag{3.4}$$

[1] Recall that the k-th term of the impulse response of a function in $\overline{B}\mathcal{H}_{\infty,\rho}(\gamma)$ is bounded by $\gamma\rho^{-k}$.

where $x \in \mathbb{R}^m$ is variable and the symmetric matrices F_i are given. The inequality symbol indicates positive definiteness (or semi-definiteness, in case of non-strict inequality). Two different LMIs $F^1(x) > 0,\ F^2(x) > 0$ may be combined as a single LMI

$$diag\ \left(F^1(x), F^2(x)\right) > 0$$

(3.4) is a convex constraint in x, *i.e.* the feasible set $\{x \,|\, F(x) > 0\}$ is a convex set. A large variety of linear and quadratic constraints arising in control and identification may be written as LMI constraints. A useful tool for converting quadratic constraints into affine constraints is Schur inequality [BGFB94]:

$$\begin{bmatrix} Q(x) & S(x) \\ S(x)^T & R(x) \end{bmatrix} > 0 \ \Leftrightarrow\ R(x) > 0,\ Q(x) - S(x)R(x)^{-1}S(x)^T > 0 \tag{3.5}$$

where $Q(x) = Q(x)^T$, $R(x) = R(x)^T$ and $S(x)$ are affine functions of the variable x.

The LMI problem we encounter in this chapter is a generalised eigenvalue problem. The general form of such problems is
minimise λ subject to $\lambda B(x) - A(x) > 0, \quad B(x) > 0,\ C(x) > 0\,.$
Here $A(x)$, $B(x)$, $C(x)$ are symmetric matrices that depend affinely on x. Efficient numerical methods exist for solving gevp and related optimisation problems, and software packages implementing such optimisation routines (such as LMI Control Toolbox from MATLAB) are commercially available.

3.3 An Algorithm to Compute Chordal Distance

An approach to solving the optimisation problem along these line is outlined below. Note that since the problem is not simultaneously convex in the v_i's and Q_i's, an iterative approach is taken. Partitioning each $X_i = \begin{bmatrix} x_{1,i} \\ x_{2,i} \end{bmatrix}$ and $v_i = \begin{bmatrix} v_{1,i} \\ v_{2,i} \end{bmatrix}$:

1. Set $k = 1$ and $Q_i^{\star,k-1} = (X_m^*(e^{j\omega_i})X_m(e^{j\omega_i}))^{-\frac{1}{2}}$ for each $i = 1, 2, \ldots, n$, where $X_{mod} := \left[\begin{smallmatrix} I \\ P_m \end{smallmatrix}\right](I - CP_m)^{-1}$ – this initial value for each $Q_{i,k-1}^{\star}$ is taken because in the case that P_t were actually P_m, it would make the argument of the infimum in (3.1) equal to zero.

2. Solve

$$\min_{\substack{v_{1,1},v_{1,2},\ldots,v_{1,n}\in\mathbb{C} \\ v_{2,1},v_{2,2},\ldots,v_{2,n}\in\mathbb{C}}} \quad \lambda \tag{3.6}$$

subject to the affine matrix inequality constraints

$$\overline{\sigma}\left(G_m(e^{j\omega_i}) - \left(X_i - \begin{bmatrix} v_{1,i} \\ v_{2,i} \end{bmatrix}\right) Q_i^{\star,k-1}\right) \leq \lambda, \tag{3.7}$$

$$\operatorname{diag}\left(\begin{bmatrix} \epsilon & \begin{bmatrix} v_{1,i} \\ v_{2,i} \end{bmatrix} \\ \begin{bmatrix} v_{1,i} \\ v_{2,i} \end{bmatrix} & \epsilon \end{bmatrix}\right) \geq 0, \tag{3.8}$$

$$\operatorname{diag}\left(\begin{bmatrix} 1 & \frac{x^*_{1,i}-v^*_{1,i}}{\gamma} \\ \frac{x_{1,i}-v_{1,i}}{\gamma} & 1 \end{bmatrix}\right) \geq 0, \tag{3.9}$$

$$\begin{bmatrix} E^{-1} & \operatorname{diag}\left(\frac{x^*_{1,i}-v^*_{1,i}}{\gamma}\right) \\ \operatorname{diag}\left(\frac{x_{1,i}-v_{1,i}}{\gamma}\right) & E \end{bmatrix} \geq 0, \tag{3.10}$$

$$\operatorname{diag}\left(\begin{bmatrix} 1 & \frac{x^*_{2,i}-v^*_{2,i}}{\gamma} \\ \frac{x_{2,i}-v_{2,i}}{\gamma} & 1 \end{bmatrix}\right) \geq 0, \tag{3.11}$$

$$\begin{bmatrix} E^{-1} & \operatorname{diag}\left(\frac{x^*_{2,i}-v^*_{2,i}}{\gamma}\right) \\ \operatorname{diag}\left(\frac{x_{2,i}-v_{2,i}}{\gamma}\right) & E \end{bmatrix} \geq 0, \tag{3.12}$$

where

$$E = \left[\frac{1}{1-\frac{e^{j(\omega_i-\omega_j)}}{\rho^2}}\right] \quad \text{for } i,j = 1,2,\ldots,n,$$

and denote by $\lambda^\star_{k,k-1}$ the minimum cost and by $v^{\star,k}_{1,i}$ and $v^{\star,k}_{2,i}$ for each $i = 1, 2, \ldots, n$ the values for each v_i at which this is achieved;

3. Given $v^{\star,k}_{1,i}$ and $v^{\star,k}_{2,i}$, solve the linear least squares problem

$$\min_{Q_i \in \mathbb{C}} \max_i \overline{\sigma}\left(G_m(e^{j\omega_i}) - \left(X_i - \begin{bmatrix} v^{\star,k}_{1,i} \\ v^{\star,k}_{2,i} \end{bmatrix}\right) Q_i\right)$$

at each frequency ω_i, denoting by $\lambda^\star_{k,k}$ the minimum cost and by $Q^{\star,k}_i$ the value Q_i at which this is achieved;

4. If $|\lambda^\star_{k,k} - \lambda^\star_{k-1,k-1}|$ is less than some tolerance then stop otherwise set $k = k+1$ and go back to step 2.

By virtue of Pick's interpolation theorem (see [DV98] for details on Pick interpolation theorem in identification), the constraints (3.9–3.12) in Step 2 above ensure the existence of analytic interpolants $f_1, f_2 : \mathbb{D} \mapsto \overline{\mathbb{D}}$ such that

$$f_1(\frac{e^{j\omega_i}}{\rho}) = \frac{x_{1,i} + v^{\star,k}_{1,i}}{\gamma} \quad \text{and} \quad f_2(\frac{e^{j\omega_i}}{\rho}) = \frac{x_{2,i} + v^{\star,k}_{2,i}}{\gamma}.$$

Correspondingly, $\hat{X}_t = \begin{bmatrix} \gamma f_1(\frac{z}{\rho}) \\ \gamma\, f_2(\frac{z}{\rho}) \end{bmatrix} \in \overline{B}\mathcal{H}_{\infty,\rho}(\gamma)$ interpolates each $X_i - \begin{bmatrix} v^{\star,k}_{1,i} \\ \\ v^{\star,k}_{2,i} \end{bmatrix}$, as required. Similar Pick interpolation based techniques have been used for worst case identification problems in [DV98]

and [CNF95]. An attractive property of the above procedure is that its cost is always non-increasing.

Lemma 2 *For $k \geq 1$,*

$$\lambda^{\star}_{k,k} \leq \lambda^{\star}_{k,k-1} \leq \lambda^{\star}_{k-1,k-1}$$

Proof : The proof follows from definition of $\lambda_{k,k-1}$ and $\lambda_{k,k}$ in Steps 2 and 3 of the above procedure and the fact that $v^{\star,k}_{1,i}$ and $v^{\star,k}_{2,i}$ are feasible solutions for the $(k+1)$-th iteration. ∎

3.4 Numerical Example

To illustrate the above procedure, consider a SISO plant

$$P_t(s) = \frac{2.1s - 2}{s^2 - 0.5s + 1.1}$$

A suboptimal loopshaping controller C designed for P_t yields $b(P_t, C) = 0.1443$. Frequency response samples ω_i at 25 frequencies, logarithmically spaced between 0.1 rad/s and 40 rad/s are used. Gaussian distributed complex noise is added to the frequency response at each frequency, with variance approximately 10% of the norm of the true frequency response at that point. These frequencies are mapped onto unit circle through bilinear transformation with sampling period $= \frac{0.9\pi}{40}$.

The problem (3.2) is solved for two models

$$P_{m1}(s) = \frac{2(s-1)}{s^2 - 0.4s + 1}$$

$$P_{m2}(s) = \frac{2(s-1)}{s^2 - 0.4s + 2}$$

The controller C stabilises both these plants with $b(P_{m1}, C) = 0.1053$ and $b(P_{m2}, C) = 0.1723$. Thus P_{m2} has a better stability margin than P_{m1} to start with. The parameters chosen for the above numerical algorithm are $\rho = 1.01$, $\gamma = 13$ and $\epsilon = 1.04$. Recall that the first two parameters may be chosen from the knowledge of impulse response; the last one may be chosen from the knowledge of the physical experiment. There is no reason in general why ϵ shouldn't be different for all frequencies; it is chosen the same here for convenience. The solid and the dashed line in fig 3.4 shows the worst case chordal distance for the models $P_{m1}(s)$ and $P_{m2}(s)$ respectively. For each model, the procedure above converges in 3 iterations. From the analysis above, it may be inferred that *any* system consistent with the *a priori* assumptions which could have produced the *a posteriori* data satisfies $\max_i \kappa(P_{m1}, P_t)(e^{j\omega_i}) \geq 0.0378$. Similarly, *any* system consistent with the *a priori* assumptions which could have produced the *a posteriori* data satisfies $\max_i \kappa(P_{m2}, P_t)(e^{j\omega_i}) \geq 0.1909$.

From this analysis, we may draw the following conclusions about suitability of the two models to represent the (unknown) true system. The chordal distance error between P_{m2} and the nearest consistent system is probably too large for P_{m2} to be useful as a model for the true system, but P_{m1} at least merits further investigation to see if it's an acceptable model for the true system.

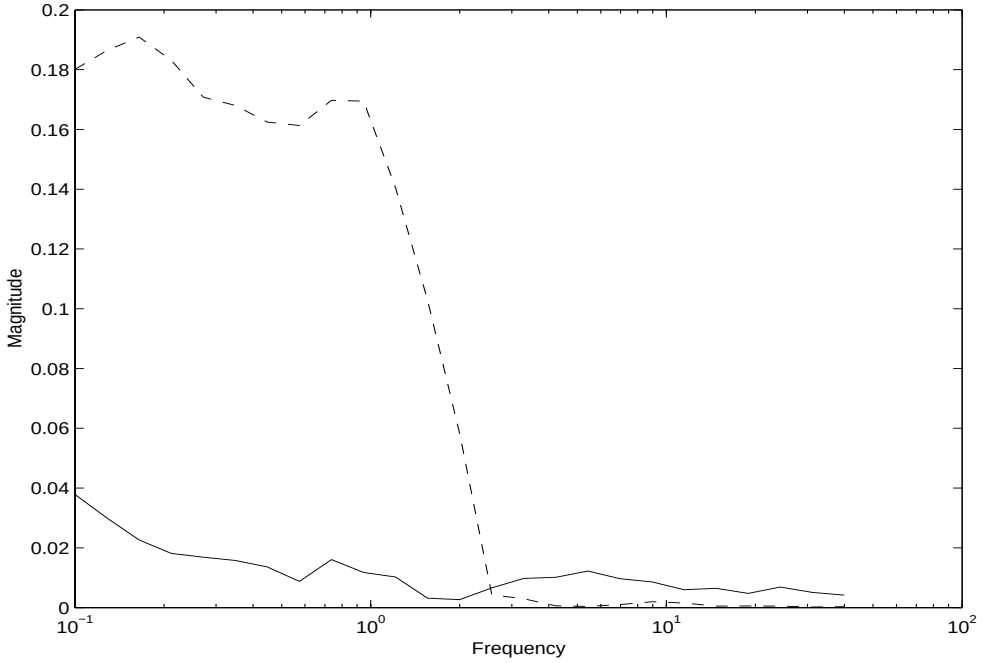

Figure 3.1: The smallest chordal distance to a system consistent with the data and a priori assumptions

Chapter 4

Pointwise Worst Case Chordal Distance from Uncertainty in Parameter Space

4.1 Introduction

The results of this chapter were first published in [BD03].

This work is a part of the wide-spread effort to connect time-domain prediction error (PE) identification (outlined in the next section) and robustness theory. In [BGS00, Bom00, BGSA01]), it was shown that PE identification with full-order model structures delivers both a model P_m for control design and an uncertainty region $\mathcal{D}$ containing the true system at a certain probability level. This uncertainty region is a set of parametrized transfer functions whose (real) parameter vector is constrained to lie in an ellipsoid. For a single input single output system, it was shown in [BGS00] that it is possible to compute the worst case (*i.e.* the largest) ν-gap between the model P_m and all plants in $\mathcal{D}$ exactly using a convex LMI based optimisation. If this worst case ν-gap is small relative to $b(P_m, C)$ for a given C, then the model-controller pair may be deemed as acceptable.

The work presented here extends the results in [BGS00] to multiple input single output (MISO) systems. An LMI based optimisation is suggested which computes the worst case ν-gap for MISO systems exactly.

The remaining chapter is organised as follows. A brief review of Prediction Error Identification is given in the next section. In Section 3, The general expression of the uncertainty region $\mathcal{D}$ delivered by PE identification in the case of a MISO true system is given. In Section 4, the concept of worst case ν-gap is defined and the new method to compute it is given. The procedure is illustrated by a numerical example in section 5.

4.2 Interlude 3: Prediction Error Identification

4.2.1 Basic Set-up

Identification is the determination on the basis of input and output, of a model within a specified set of models, which best approximates the input-output behaviour of the system under test. A technique called Prediction Error identification is briefly introduced here. Consider a closed loop system as shown in fig.(1.1) again. The following assumptions are made about the system:

1. The reference signal $r(t)$ is quasi-stationary [Lju99], i.e. it is either a stationary stochastic process or a bounded deterministic sequence such that the limits

$$R_r(\tau) = \lim_{N\to\infty} \frac{1}{N} \sum_{t=1}^{N} r(t) r^T(t-\tau)$$

   exist for all τ.

2. $w_i(t) = L_i(q) e_i(t),\ i = 1, 2$ where L_i are monic and inversely stable linear filters and e_i are a stationary zero mean white processes having bounded moments of order $4 + l$, $l > 0$.

$$E e_{i,k}\, e_{j,s}^T = \Lambda \delta(t-s)$$

   where $\delta(\cdot)$ is Dirac delta function.

3. The plant P is strictly proper, $P(0) = 0$.

4. The controller C is linear and the loop is asymptotically stable.

Note that open loop identification of a stable plant is simply a special case of the above set-up, with $C = 0$.

4.2.2 The Method

An approach considered here disregards presence of feedback and identifies a model *directly* from its input-output data.

Some formal definitions are first needed. Define a set of monic and inversely stable filters:

$$\mathcal{L} = \{\, L \,|\, L \in \mathcal{R},\, L^{-1} \in \mathcal{RH}_\infty\,,\, L(0) = I \}.$$

Here, $\mathcal{R}$ is a set of finite dimensional systems and $\mathcal{RH}_\infty = \mathcal{R} \cap \mathcal{H}_\infty$. Next, define a set of *ordered pairs* (L, P) of transfer matrices :

$$\mathcal{LP} = \{\, (L, P) \,|\, L \in \mathcal{L},\, P \in \mathcal{R},\, P(0) = 0,\, L^{-1}P \in \mathcal{RH}_\infty \}.$$

Then a *model structure* is a differentiable mapping from a connected and open subset of n dimensional parameter space $\mathbb{R}^n$ to a subset $\mathcal{LP}_A$ of $\mathcal{LP}$,

$$\mu : \mathbb{R}^n \supseteq D_\mu \to \mathcal{LP}_A \subseteq \mathcal{LP},\ \mu(\theta) = (\, L(q,\theta),\ P(q,\theta)\,)$$

such that the gradient $\frac{\partial}{\partial\theta}\begin{bmatrix}L(q,\theta) & P(q,\theta)\end{bmatrix}$ is stable. This model structure is used to describe the relationship between the measurable input $u(t)$ and measured output $y(t)$ as

$$y(t) = P(q,\theta)u(t) + L(q,\theta)e(t) \tag{4.1}$$

where $e(t)$ is a zero mean white process. q is a backward shift operator.

Define one-step ahead prediction error for a model structure μ at a parameter vector (θ^*) and at sample time t by

$$\epsilon(t,\mu(\theta^*)) = y(t) - \hat{y}(t|\mu(\theta^*)) \tag{4.2}$$

where $\hat{y}(t|\mu(\theta^*))$ is a one-step ahead prediction of the output based on the data up to sample time $t-1$. To find an optimal one-step ahead prediction, (4.1) is rewritten as

$$y(t) = [I - L^{-1}(q,\theta^*)]y(t) + L^{-1}(q,\theta^*)P(q,\theta^*)u(t) + e(t). \tag{4.3}$$

For a sufficiently large t (i.e. barring the starting up of the IIR filters from zero initial conditions), all the terms on the right hand side except the disturbance $e(t)$ are determined from the past data up to $y(t-1)$. It may be shown that the following choice of one-step ahead prediction minimises the variance of the prediction error $\epsilon(t,\mu(\theta^*))$ [Lju99] :

$$\hat{y}(t|\mu(\theta^*)) = [I - L^{-1}(q,\theta^*)]\, y(t) + L^{-1}(q,\theta^*)P(q,\theta^*)u(t). \tag{4.4}$$

Restricting (L,P) to $\mathcal{LP}$ ensures that the above one-step ahead predictor is stable. Let

$$Z^N = [y(1)\ u(1)\ y(2)\ u(2)\ \cdots y(N)\ u(N)]. \tag{4.5}$$

For this data set and a model structure $\mu(\theta)$, the parameter estimate $\hat{\theta}_N$ is defined by

$$V_N(\mu(\hat{\theta}_N), Z^N) = \min_{\theta\in D_\mu} V_N(\mu(\theta), Z^N) \tag{4.6}$$

where

$$V_N(\mu(\theta), Z^N) = \text{trace}\left(\frac{1}{N}\sum_{t=1}^{N}\epsilon(t,\mu(\theta))\epsilon^T(t,\mu(\theta))\right). \tag{4.7}$$

The optimisation problem (4.6) is usually solved by some modified variant of Gauss-Newton method [Fle87]. Under certain assumptions, this method also yields information regarding uncertainty in the obtained model in terms of a covariance matrix of parameter estimates. The purpose of the work that follows in this chapter is to map this uncertainty into chordal distance uncertainty.

4.3 Uncertainty Region for MISO systems

In this section, an expression of the uncertainty regions $\mathcal{D}$ delivered by PE identification of MISO true systems in a full order model structure [Lju99] is given. The ensuing discussion will focus on

MISO systems with two inputs for notational simplicity. However all the results are applicable for any (finite) number of inputs. Assume thus that the true system is linear and time-invariant, with a rational MISO transfer function P_t such that

$$y = \overbrace{\begin{pmatrix} P_{0,1} & P_{0,2} \end{pmatrix}}^{P_t} \overbrace{\begin{pmatrix} u_1 \\ u_2 \end{pmatrix}}^{u} + v$$

where v is additive noise. It is assumed that the identification is performed using a parametrization of P_t with an identical auto-regressive part for $P_{0,1}$ and $P_{0,2}$ i.e.

$$P_t = P(z, \delta_0) = \frac{\begin{pmatrix} e_1 + Z_{N_1}\delta_0 & e_2 + Z_{N_2}\delta_0 \end{pmatrix}}{1 + Z_D\delta_0} \tag{4.8}$$

where $\delta_0 \in \mathbf{R}^{k\times 1}$ is the *unknown* true parameter vector, $Z_{N_1}(z)$, $Z_{N_2}(z)$ and $Z_D(z)$ are row vectors of size k of known transfer functions. $e_1(z)$ and $e_2(z)$ are known transfer functions. This is the case when P_t (and the noise model) has an ARX structure or an ARMAX structure. This is also the case when $P_{0,1}$ (resp. $P_{0,2}$) is parametrized by the sum of a given model $e_1(z)$ (resp. $e_2(z)$) and an expansion of linear basis functions (such as Laguerre filters). In this last case, $Z_D = 0$.

When $P_{0,1} = n_{0,1}/d_{0,1}$ and $P_{0,2} = n_{0,2}/d_{0,2}$ [1] have different auto-regressive parts, a structure such as in (4.8) can be obtained by considering a parametrization $P(z, \delta_0)$ such that $Z_{N_1}\delta_0 = n_{0,1}\ d_{0,2}$, $Z_{N_2}\delta_0 = n_{0,2}\ d_{0,1}$ and $1 + Z_D\delta_0 = d_{0,1}\ d_{0,2}$. Here $e_1(z)$ and $e_2(z)$ are equal to 0.

Proposition 1 *Consider $P_t = P(z, \delta_0)$, the true MISO system with two inputs parametrized as in (4.8). A PE identification experiment (with a full order model structure) performed on P_t delivers an identified model $P_m = P(z, \hat{\delta})$ and an uncertainty region $\mathcal{D}$ containing the true system P_t at a prescribed probability level α. This uncertainty region is centered at $P(z, \hat{\delta})$ and can be described by the following generic form:*

$$\mathcal{D} = \left\{ P(z,\delta) \mid P(z,\delta) = \frac{\begin{pmatrix} e_1 + Z_{N_1}\delta & e_2 + Z_{N_2}\delta \end{pmatrix}}{1 + Z_D\delta} \text{ and } \delta \in U \right\} \tag{4.9}$$

where $U = \{\delta \mid (\delta - \hat{\delta})^T R(\delta - \hat{\delta}) < \chi^2\}$, $\delta \in \mathbf{R}^{k\times 1}$ is a real parameter vector, $\hat{\delta}$ is the estimated parameter vector defining the identified model, R is a symmetric positive definite matrix $\in \mathbf{R}^{k\times k}$ that is equal to the inverse of the covariance matrix of $\hat{\delta}$, χ^2 is determined by the desired probability level α, $Z_{N_1}(z)$, $Z_{N_2}(z)$ and $Z_D(z)$ are row vectors of size k of known transfer functions. $e_1(z)$ and $e_2(z)$ are known transfer functions.

Proof Trivial extension of the results in [Bom00]. ∎

Note that different identification experiments (i.e. open-loop or closed-loop identification, different measured data, ...) lead to different identified parameter vectors, different covariance matrices, and therefore also different uncertainty sets $\mathcal{D}$.

[1] Here, $n_{0,i}(z)$ and $d_{0,i}(z)$ are the numerator and denominator of $P_{0,i}$, respectively.

Due to the multivariable structure in (4.9), the numerical method that was developed [BGS00] for a SISO uncertainty region in order to compute the worst case $\nu-$gap for $\mathcal{D}$ is no more valid. In the ensuing sections, a new numerical methodology adapted to the multivariable structure of $\mathcal{D}$ will be presented in order to compute this measure.

4.4 An Algorithm to Compute the Worst Case Chordal Distance for $\mathcal{D}$

As said in the introduction, the robust stability measure for the uncertainty region $\mathcal{D}$ is based on the concept of *worst-case ν-gap* between the identified model $P_m = P(z, \hat{\delta})$ and the uncertainty set $\mathcal{D}$ that has been introduced in [BGS00]. The worst-case ν-gap is an extension of the ν-gap, introduced by Vinnicombe [Vin93a], which is a measure of distance between two transfer functions.

Consider the uncertainty region $\mathcal{D}$ given in Proposition 1 and centered at the identified model $P_m = P(z, \hat{\delta})$. The worst case ν-gap $\delta_{WC}(P_m, \mathcal{D})$ is given by:

$$\delta_{WC}(P_m, \mathcal{D}) = \sup_{P_{in} \in \mathcal{D}} \delta_\nu(P_m, P_{in}) \tag{4.10}$$

where $\delta_\nu(P_m, P_{in})$ is the ν-gap between the plants P_m and P_{in} (see [Vin93a]).

The definition of another important quantity is also recalled: the worst case chordal distance $\kappa_{WC}(P_m(e^{j\omega}), \mathcal{D})$. This quantity, whose computation is the result of a convex optimisation problem involving LMI constraints in the MISO case as will be shown in Section 4.4, will allow us to give an alternative expression for $\delta_{WC}(P_m, \mathcal{D})$.

At a particular frequency ω, define $\kappa_{WC}(P_m(e^{j\omega}), \mathcal{D})$ as the maximum chordal distance between $P_m(e^{j\omega})$ and the frequency responses of all plants in $\mathcal{D}$ at this frequency:

$$\kappa_{WC}(P_m(e^{j\omega}), \mathcal{D}) = \sup_{P_{in} \in \mathcal{D}} \kappa(P_m(e^{j\omega}), P_{in}(e^{j\omega})) \tag{4.11}$$

where the chordal distance κ is defined as in (2.3).

This last quantity can now be used to give an alternative expression of the worst case $\nu-$gap. This is done in the following lemma, which is an extension of a property presented in [Vin93b, page 66].

Lemma 3 *The worst case Vinnicombe distance $\delta_{WC}(P_m, \mathcal{D})$ defined in (4.10) can also be expressed in the following way using the worst case chordal distance:*

$$\delta_{WC}(P_m, \mathcal{D}) = \sup_{\omega} \kappa_{WC}(P_m(e^{j\omega}), \mathcal{D}) \tag{4.12}$$

where $\kappa_{WC}(P_m(e^{j\omega}), \mathcal{D})$ is defined in (4.11).

Proof: See [BGS00]. ∎

Recall the definition of the worst case ν-gap between the model P_m and all plants in an uncertainty region $\mathcal{D}$. In this subsection, a procedure to compute this worst case ν-gap $\delta_{WC}(P_m, \mathcal{D})$ in

the considered case of an uncertainty region delivered by the PE identification of a MISO true system P_t is given. This LMI-procedure is the extension to the MISO case of the procedure developed in [BGS00] for the SISO systems.

Theorem 1 *Consider the uncertainty region $\mathcal{D}$ given in Proposition 1 and centered at the identified model $P_m = P(z, \hat{\delta})$. Then $\kappa_{WC}(P_m(e^{j\omega}), \mathcal{D}) = \sqrt{\gamma_{opt}}$, where γ_{opt} is the optimal value of γ in the following standard convex optimisation problem involving LMI constraints [BGFB94] evaluated at ω:*

$$\begin{array}{ll} \textit{minimise} & \gamma \\ \textit{over} & \gamma,\ \tau \\ \textit{subject to} & \tau \geq 0 \textit{ and} \end{array}$$

$$\begin{pmatrix} Re(a_{11}) & Re(a_{12}) \\ Re(a_{12}^*) & Re(a_{22}) \end{pmatrix} - \tau \begin{pmatrix} R & -R\hat{\delta} \\ (-R\hat{\delta})^T & \hat{\delta}^T R \hat{\delta} - \chi^2 \end{pmatrix} < 0 \tag{4.13}$$

where

- $a_{11} = \left(\ (k_1 Z_1^* + k_2 Z_2^*) Z_1 + (k_2^* Z_1^* + k_3 Z_2^*) Z_2 \ \right) - \gamma \left(\ Z_{N_1}^* Z_{N_1} + Z_{N_2}^* Z_{N_2} + Z_D^* Z_D \ \right),$
- $a_{12} = \left(\ f_1 (k_1 Z_1^* + k_2 Z_2^*) + f_2 (k_2^* Z_1^* + k_3 Z_2^*) \ \right) - \gamma \left(\ e_1 Z_{N_1}^* + e_2 Z_{N_2}^* + Z_D^* \ \right),$
- $a_{22} = \left(\ f_1 (k_1 f_1^* + k_2 f_2^*) + f_2 (k_2^* f_1^* + k_3 f_2^*) \ \right) - \gamma \left(\ 1 + e_1 e_1^* + e_2 e_2^* \ \right),$
- $f_1 = x_1 - e_1$ *and* $f_2 = x_2 - e_2$
- $Z_1 = x_1 Z_d - Z_{N_1}$ *and* $Z_2 = x_2 Z_d - Z_{N_2}$
- $\begin{pmatrix} k_1 & k_2 \\ k_2^* & k_3 \end{pmatrix} = BB^*$ *with* $B = \left(\ I_2 + X^* X \ \right)^{-\frac{1}{2}}$
- $X = \begin{pmatrix} x_1 & x_2 \end{pmatrix} = P_m(e^{j\omega}).$

The worst case ν-gap is then obtained as

$$\delta_{WC}(P_m, \mathcal{D}) = \sup_{\omega} \kappa_{WC}(P_m(e^{j\omega}), \mathcal{D})$$

Proof We prove that the square root of the solution of the LMI optimisation problem gives the worst case chordal distance $\kappa_{WC}(P_m(e^{j\omega}), \mathcal{D})$ at some frequency ω. The derivation of the worst case ν-gap is a direct consequence of Lemma 3.

If the frequency response of the model $P_m(e^{j\omega})$ is denoted by X, and that of any plant $P(e^{j\omega}, \delta) \in \mathcal{D}$ by $Y(\delta)$. Then a convenient way to state the problem of computing the worst case chordal distance at some frequency ω is as follows:

$$\textit{minimise } \gamma \textit{ such that}$$
$$\kappa(X, Y(\delta))^2 < \gamma \textit{ for all } \delta \in U$$

Let us rewrite $\kappa(X, Y(\delta))^2$ in an appropriate way for the LMI formulation. Using the fact that X and $Y(\delta)$ are in $\mathcal{C}^{1\times 2}$, the fact that $\overline{\sigma}^2(A) = \overline{\lambda}(A^*A)$ ($\overline{\lambda}(A^*A)$ is the largest eigenvalue of A^*A) and the definition (2.3) of $\kappa(X, Y(\delta))$:

$$\kappa(X, Y(\delta)) = \overline{\sigma}\left((1 + Y(\delta)Y(\delta)^*)^{-\frac{1}{2}}(X - Y(\delta)) \overbrace{(I_2 + X^*X)^{-\frac{1}{2}}}^{B} \right),$$

we obtain successively that

$$\kappa(X, Y(\delta))^2 < \gamma \Longleftrightarrow$$

$$(1 + Y(\delta)Y(\delta)^*)^{-1} \ \overline{\lambda}\Big(\ B^*(X - Y(\delta))^*(X - Y(\delta))B \ \Big) < \gamma \Longleftrightarrow$$

$$(X - Y(\delta))BB^*(X - Y(\delta))^* < \gamma(1 + Y(\delta)Y(\delta)^*) \tag{4.14}$$

where the last equivalence is a consequence of the fact that, when ϕ is a row vector, $\overline{\lambda}(\phi^*\phi) = \phi\phi^*$. By pre-multiplying (4.14) by $d_Y \stackrel{\Delta}{=} (1 + Z_D\delta)$ and post-multiplying the same expression by d_Y^*, we obtain:

$$(d_Y X - N_Y)BB^*(d_Y^*X^* - N_Y^*) < \gamma(d_Y d_Y^* + N_Y N_Y^*) \tag{4.15}$$

where $N_Y = \Big(\ e_1 + Z_{N_1}\delta \qquad e_2 + Z_{N_2}\delta \ \Big)$. Using the notations used in the statement of Theorem 1, Expression (4.15) is equivalent with:

$$\begin{pmatrix} f_1 + Z_1\delta & f_2 + Z_2\delta \end{pmatrix} \begin{pmatrix} k_1 & k_2 \\ k_2^* & k_3 \end{pmatrix} \begin{pmatrix} f_1 + Z_1\delta & f_2 + Z_2\delta \end{pmatrix}^* \\ < \gamma(d_Y d_Y^* + N_Y N_Y^*)$$

Some trivial manipulations show then that this last expression is equivalent with the following constraint on δ with variable γ:

$$\begin{pmatrix} \delta \\ 1 \end{pmatrix}^* \begin{pmatrix} a_{11} & a_{12} \\ a_{12}^* & a_{22} \end{pmatrix} \begin{pmatrix} \delta \\ 1 \end{pmatrix} < 0 \tag{4.16}$$

with a_{11}, a_{12} and a_{22} as defined in the statement of Theorem 1. Since δ is real, it can be shown that (4.16) is equivalent with

$$\overbrace{\begin{pmatrix} \delta \\ 1 \end{pmatrix}^T \begin{pmatrix} Re(a_{11}) & Re(a_{12}) \\ Re(a_{12}^*) & Re(a_{22}) \end{pmatrix} \begin{pmatrix} \delta \\ 1 \end{pmatrix}}^{\psi(\delta)} < 0 \tag{4.17}$$

This last expression is equivalent to stating that $\kappa(P_m(e^{j\omega}), P(e^{j\omega}, \delta))^2 < \gamma$ for a particular $\delta \in U$. However, this must be true for all $\delta \in U$. Therefore, (4.17) must be true for all δ such that:

$$\overbrace{\begin{pmatrix} \delta \\ 1 \end{pmatrix}^T \begin{pmatrix} R & -R\hat{\delta} \\ (-R\hat{\delta})^T & \hat{\delta}^T R\hat{\delta} - \chi^2 \end{pmatrix} \begin{pmatrix} \delta \\ 1 \end{pmatrix}}^{\rho(\delta)} < 0 \tag{4.18}$$

which is equivalent to the statement "$\delta \in U$". Let us now recapitulate. Computing $\kappa_{WC}(P_m(e^{j\omega}), \mathcal{D})^2$ is equivalent to finding the smallest γ such that $\psi(\delta) < 0$ for all δ for which $\rho(\delta) < 0$. By the $\mathcal{S}$ procedure [BGFB94], this problem is equivalent to finding the smallest γ and a positive scalar τ such that $\psi(\delta) - \tau\rho(\delta) < 0$, for all $\delta \in \mathbf{R}^{k\times 1}$ which is precisely (4.13). To complete this proof, note that the worst case chordal distance at ω is thus equal to $\sqrt{\gamma_{opt}}$ where γ_{opt} is the optimal value of γ. ■

Some comments on this result are in order.

- The LMI-procedure given in Theorem 1 for a MISO system with two inputs can be easily extended to all MISO systems. Theorem 1 can also be easily adapted to SIMO systems i.e. single-input multiple-outputs systems. For two SIMO systems P_1 and P_2, $P_1^T(e^{j\omega})$ and $P_2^T(e^{j\omega})$ are indeed row vectors and $\kappa(P_1(e^{j\omega}), P_2(e^{j\omega})) = \kappa(P_1^T(e^{j\omega}), P_2^T(e^{j\omega}))$. Finally, Theorem 1 allows us also to compute frequency weighted worst case ν-gap : $\delta_{WC}^{\alpha}(P_m, \mathcal{D}) = \sup_{P_{in}\in\mathcal{D}} \delta_\nu(\alpha P_m, \alpha P_{in})$ where α is a (scalar) transfer function. This especially makes sense in the $\mathcal{H}_\infty$ loopshaping design paradigm, where $\alpha(z)$ would be a weighting function (see [GM89] for details). The weighting α in this case would only modify e_1, e_2, Z_{N_1}, Z_{N_2} and as such would not have an effect on the suggested algorithm.

- In the $\mathcal{H}_\infty$ loopshaping design paradigm, the performance of a closed-loop system $[C\ P]$ is measured by its generalized stability margin $b(P, C)$ (defined in (2.4)). In that sense, the worst case ν-gap $\delta_{WC}(P_m, \mathcal{D})$ can be seen as a measure of the worst case performance degradation in the set $\mathcal{D}$. Indeed, given any controller C which stabilises all plants in $\mathcal{D}$, we have the following result: $\inf_{P\in\mathcal{D}} b(P, C) \geq b(P_m, C) - \delta_{WC}(P_m, \mathcal{D})$. This result is a direct consequence of the properties of the ν-gap metric [Vin93b] and of the fact that $\mathcal{D}$ is embedded in the ν-gap uncertainty region $\{P|\delta_\nu(P_m, P) \leq \delta_{WC}(P_m, \mathcal{D})\}$. Note that, in practice, in $\mathcal{H}_\infty$ loopshaping design, a shaped nominal plant should be considered and thus this result has to be rewritten with this shaped plant and with a *frequency weighted* worst case ν-gap .

4.5 Numerical Example

Let us now illustrate our results by an example. Consider thus the following MISO true system in the ARX structure:

$$y(t) = \frac{\overbrace{\begin{pmatrix} n_{0,1}(z) & n_{0,2}(z) \end{pmatrix}}^{P_t}}{d_0(z)} u(t) + \frac{e(t)}{d_0(z)}$$

where $e(t)$ is a white noise of variance 0.1, $n_{0,1} = 0.1047z^{-1} + 0.0872z^{-2}$, $n_{0,2} = 0.2z^{-1} + 0.05z^{-2}$ and $d_0 = 1 - 1.5578z^{-1} + 0.5769z^{-2}$. A PE identification experiment is performed on this true system using an input signal whose two components are a white noise of variance 1. 5000 data are collected and the following model is identified:

$$P_m = P(z, \hat{\delta}) = \frac{\begin{pmatrix} 0.099z^{-1} + 0.086z^{-2} & 0.2013z^{-1} + 0.048z^{-2} \end{pmatrix}}{1 - 1.5554z^{-1} + 0.578z^{-2}}$$

Along with this model, the uncertainty region $\mathcal{D}$ centered at P_m and containing the true system P_t at a probability 0.95 is built. This uncertainty region has the general structure (4.9) with $e1$ and $e_2 = 0$, $\chi^2 = 12.6$, $Z_D = (z^{-1}\ z^{-2}\ 0\ 0\ 0\ 0)$, $Z_{N_1} = (0\ 0\ z^{-1}\ z^{-2}\ 0\ 0)$, $Z_{N_2} = (0\ 0\ 0\ 0\ z^{-1}\ z^{-2})$ and $\hat{\delta} = (-1.554, 0.578, 0.099, 0.086, 0.2013, 0.048)^T$.

The worst case chordal distance $\kappa_{WC}(P_m(e^{j\omega}), \mathcal{D})$ is at each frequency using the LMI tools developed in Section 4.4. The worst case chordal distances are represented in Figure 4.5 where they are compared with the actual chordal distances $\kappa(P_m(e^{j\omega}), P_t(e^{j\omega}))$ between the identified model P_m and the true system P_t (which is spuposed to be unknown).

According to Lemma 3, the worst case ν-gap $\delta_{WC}(P_m, \mathcal{D})$ can be derived from the worst chordal distances: $\delta_{WC}(P_m, \mathcal{D}) = \sup_\omega \kappa_{WC}(P_m(e^{j\omega}), \mathcal{D}) \approx 0.0716$.

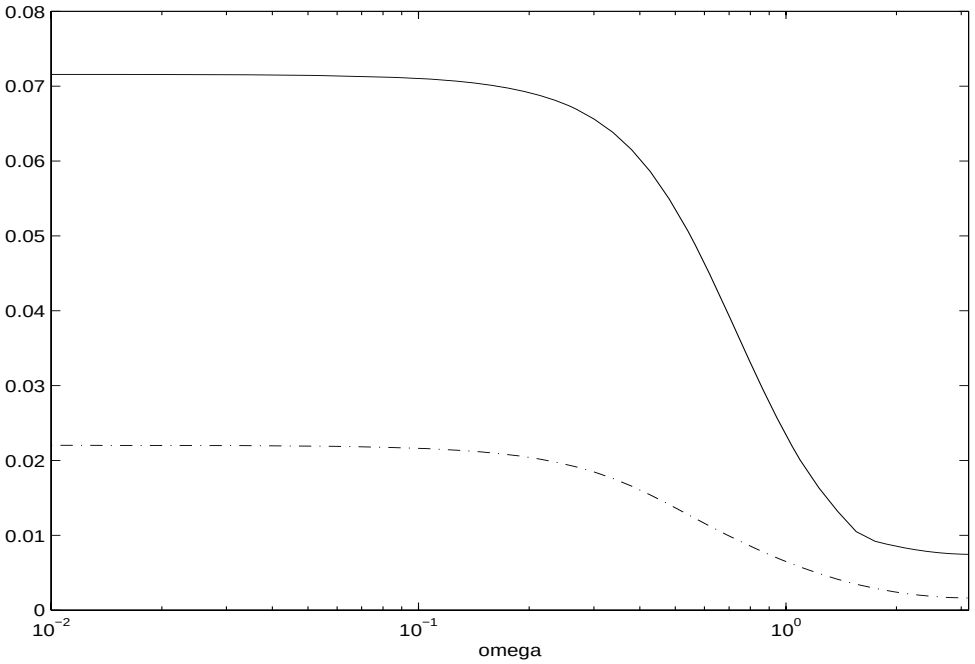

Figure 4.1: $\kappa_{WC}(P_m(e^{j\omega}), \mathcal{D})$ (solid) and $\kappa(P_m(e^{j\omega}), P_t(e^{j\omega}))$ (dashdot) at each frequency

Chapter 5

A Lower Bound on The Achieved Closed Loop Performance from A Finite Data

The results of this chapter were first published in [DC03a].

Recall the lower bound in (2.7)

$$b(P_t, C) \geq \inf_{\omega} \Big(\rho(P_m, C)(e^{j\omega}) - \kappa(P_m, P_t)(e^{j\omega}) \Big).$$

Suppose, the true plant frequency response $P_t(e^{j\omega_i})$ is known to lie within a known chordal distance from the frequency response of the model $P_m(e^{j\omega_i})$ at a finite number of frequencies $\{\omega_0, \omega_1, \omega_2, \ldots, \omega_m\}$. This information may *e.g.* be result of an optimisation procedure described in the earlier chapter. Then provided the frequency responses of P_m, P_t and C_n are 'sufficiently smooth' and the frequency grid is 'sufficiently dense', the infimum over the continuum of frequencies in the lower bound of (2.7) may be approximated by an infimum over the finite set $\{\omega_i\}$:

$$\inf_{\omega} \Big(\rho(P_m, C)(e^{j\omega}) - \kappa(P_t, P_m)(e^{j\omega}) \Big) \approx \min_{i} \Big(\rho(P_m, C)(e^{j\omega_i}) - \kappa(P_t, P_m)(e^{j\omega_i}) \Big)$$

Here, a lower bound on the right-hand side of (2.7) is derived by using an appropriate notion of smoothness and a finite set of frequency response data. The quantity used to capture the smoothness of frequency responses, in terms of the variation in chordal distance, is defined by

$$V_P = \|\tilde{G}_P G_P'\|_\infty, \tag{5.1}$$

where $G_P' = \frac{dG_P}{dz}$. As shown in [Vin96], given two frequencies ω_1 and ω_2,

$$\kappa(P(e^{j\omega_1}), P(e^{j\omega_2})) \leq V_P |\omega_1 - \omega_2|.$$

Given P, it is not difficult to compute V_P. First, $G_P, \tilde{G}_P$ can be computed using by well-known techniques which are available in standard software such as MATLAB. Then given $G_P = H(zI - A)^{-1}F + D$ (where $\{A, F, H, D\}$ is any state space realisation of G_P), it follows that $G_P' = S_1 S_2$

where $S_1 = -H(zI - A)^{-1}I$ and $S_2 = I(zI - A)^{-1}F$. That is, V_P is simply the infinity norm of a product of three transfer functions all of which may be easily derived from P. Below, a lower bound on $\rho(P_t, C)$ at any intermediate frequency $\omega_\star \in [\omega_i, \omega_{i+1}]$ is obtained using the definition of V_P.

Proposition 2 *Let C be a controller that stabilises both the true plant P_t and the model P_m. Then for any $\omega_\star \in [\omega_i, \omega_{i+1}]$ the following inequality holds:*

$$\rho(P_t, C)(e^{j\omega_\star}) \;\geq\; \left(\max \left\{ b(P_m, C), \sqrt{1 - x_i^2} \right\} - y_i \right) \tag{5.2}$$

where

$$x_i \;:=\; \min \left\{ \kappa(P_m, -C^*)(e^{j\omega_i}) \,,\, \kappa(P_m, -C^*)(e^{j\omega_{i+1}}) \right\} + (V_{P_m} + V_{-C^*})|\omega_{i+1} - \omega_i|, \tag{5.3}$$

$$y_i \;:=\; \min \left\{ \kappa(P_m, P_t)(e^{j\omega_i}) \,,\, \kappa(P_m, P_t)(e^{j\omega_{i+1}}) \right\} + (V_{P_t} + V_{P_m})|\omega_{i+1} - \omega_i| \tag{5.4}$$

and V_P is as defined in (5.1).

Proof : Given P, it can be shown that

$$\rho(P, C)(e^{j\omega}) = \sqrt{1 - \kappa^2(P, -C^*)(e^{j\omega})} \tag{5.5}$$

at all frequencies [Vin93a]. Hence, it follows from (2.6) that

$$\rho(P_t, C)(e^{j\omega_\star}) \;\geq\; \sqrt{1 - \kappa^2(P_t, -C^*)(e^{j\omega_\star})} - \kappa(P_t, P_m)(e^{j\omega_\star})$$

The lower bound claimed follows by bounding, from above, each of the two chordal distances terms shown. Since $\kappa(\cdot, \cdot)$ is a metric [Vin01], it follows by the triangle inequality,

$$\begin{aligned} \kappa(P_m, P_t)(e^{j\omega_\star}) \;&\leq\; \kappa(P_m(e^{j\omega_\star}), P_m(e^{j\omega_i})) + \kappa(P_m(e^{j\omega_i}), P_t(e^{j\omega_i})) + \kappa(P_t(e^{j\omega_i}), P_t(e^{j\omega_\star})) \\ &\leq\; \kappa(P_m(e^{j\omega_i}), P_t(e^{j\omega_i})) + (V_{P_m} + V_{P_t})\,|\omega_\star - \omega_i|. \end{aligned} \tag{5.6}$$

Similarly,

$$\kappa(P_m, P_t)(e^{j\omega_\star}) \;\leq\; \kappa(P_m(e^{j\omega_{i+1}}), P_t(e^{j\omega_{i+1}})) + (V_{P_m} + V_{P_t})\,|\omega_\star - \omega_{i+1}|. \tag{5.7}$$

Note that the upper bound y_i on $\kappa(P_m, P_t)(e^{j\omega_\star})$ in (5.3) is simply a consequence of equations (5.6-5.7). The upper bound x_i on $\kappa(P_m, -C^*)(e^{j\omega_\star})$ in (5.4) follows in a similar manner. The result now follows by using equation (5.5) and the fact that both $b(P_m, C)$ and $\sqrt{1 - x_i^2}$ are lower bounds on $\rho(P_m, C)(e^{j\omega_\star})$. ∎

When the right hand side in (5.2) is positive for all i, Lemma 1 further suggests that

$$\begin{aligned} b(P_t, C) \;&:=\; \inf_{\omega} \rho(P_t, C)(e^{j\omega}) \\ &=\; \min_i \inf_{\omega \in [\omega_i, \omega_{i+1}]} \rho(P_t, C)(e^{j\omega}) \\ &\geq\; \min_i \left(\max \left\{ b(P_m, C), \sqrt{1 - x_i^2} \right\} - y_i \right). \end{aligned} \tag{5.8}$$

Note that the right-hand side of (5.8) is a lower bound for the right-hand side of (2.7), as discussed at the end of the previous section. Furthermore, observe that all terms in this lower bound (except V_{P_t}) are either known or can be computed from the measured data. Although the complexity of P_t is unlikely to be known exactly, one may incorporate an 'educated guess' into the *a priori* information; *e.g.* P_t may be allowed to be *at most twice as complex* as its model P_m (*i.e.* $V_{P_t} \leq 2V_{P_m}$). In addition to being computationally tractable, the effect of complexity on achieved worst case performance is clearly visible in this new bound. In particular,

- The frequency separation $|\omega_{i+1} - \omega_i|$ should be small wherever $\kappa(P_m, P_t)(e^{j\omega_i})$ is large and/or $\rho(P_m, C)$ is small. This will reduce the effect of complexity terms on the bound.
- An increase in the complexity of plant or model or controller worsens the lower bound on achieved performance. If this lower bound is poor, one may consider re-designing a controller with lower complexity (*e.g.* using the technique suggested in [Vin96]) or obtaining a plant model P_m with lower complexity.

To conclude, it is interesting to consider more closely the term V_{-C^*} in (5.3), which was simply considered to be a measure of controller complexity, without explanation. Note that it is not clear that $V_{-C^*} = V_C$ in general. However, by considering the behaviour of frequency-domain symbols on the unit circle only, and since in this case $\tilde{G}_C^*$ and G_C^* can be considered to be normalised graph symbols (now left and right invertible in $\mathcal{L}_\infty$) of $-C^*$, it follows that

$$V_{-C^*} = \|\tilde{G}_{-C^*}(G_{-C^*})'\|_\infty = \|G_C^*(\tilde{G}_C^*)'\|_\infty = \|\tilde{G}_C' G_C\|_\infty =: \tilde{V}_C,$$

where the norms here all correspond to the one on $\mathcal{L}_\infty$, and the third equality holds because given an $X \in \mathcal{RL}_\infty$, $-z^2(X^*)' = (X')^*$ and $\|\frac{-1}{z^2}X\|_\infty = \|X\|_\infty = \|X^*\|_\infty$. Hence, mimicking the proof of Lemma 5.4 in [Vin01], it also follows that

$$\kappa(C(e^{j\omega_1}), C(e^{j\omega_2})) \leq \tilde{V}_C|\omega_1 - \omega_2|.$$

That is, $\tilde{V}_C$ can be thought of as measuring the complexity of C in the same way as V_C. In fact, for a single-input single-output C, or a diagonal multiple-input multiple-output C, it may be easily shown that $\tilde{V}_C = V_C$.

∘ ∘ ∘

Bibliography

[BD03] X. Bombois and P. Date. Connecting PE identification and robust control theory: The multiple-input single-output case. part I: Uncertainty region validation. In *Proc. of SYSID*, Rotterdam, The Netherlands, 2003.

[BGFB94] S. Boyd, L.El Ghaoui, E. Feron, and V. Balakrishnan. *Linear Matrix Inequalities in System and Control Theory*. SIAM, 1994.

[BGS00] X. Bombois, M. Gevers, and G. Scorletti. A measure of robust stability for a set of parametrized transfer functions. *IEEE Trans. Automat. Contr.*, 2000.

[BGSA01] X. Bombois, M. Gevers, G. Scorletti, and B.D.O. Anderson. Robustness analysis tools for an uncertainty set obtained by prediction error identification. *Automatica*, 37:1692–1636, 2001.

[Bom00] X. Bombois. *Connecting Prediction Error Identification and Robust Control Analysis: a new framework*. PhD thesis, Université Catholique de Louvain., 2000.

[CNF95] J. Chen, C.N. Nett, and M.K.H. Fan. Worst case system identification in $\mathcal{H}_\infty$: Validation of a priori information, essentially optimal algorithms, and error bounds. *IEEE Trans. Automat. Contr.*, 40:1260–1265, 1995.

[CV02] M. Cantoni and G. Vinnicombe. Linear feedback systems and the graph topology. *IEEE Trans. Automat. Contr.*, 47(5):710–719, 2002.

[DC03a] P. Date and M. Cantoni. A lower bound on achieved closed-loop performance from finite data. In *Proc. of European Contr. Conf.*, Cambridge, U.K., 2003. to be published.

[DC03b] P. Date and M. Cantoni. Validation of closed-loop behaviour from noisy frequency response measurements. In *Proc. of European Contr. Conf.*, Cambridge, U.K., 2003. to be published.

[Dow01] A. Dowling. private communication, 2001.

[DV98] P. Date and G. Vinnicombe. New untuned algorithms for identification in $\mathcal{H}_\infty$. In *Proc. of 37th Conf. on Des. and Control*, Tampa, USA, 1998.

[ES85] A. K. El-Sakkary. The gap metric: Robustness of stabilization of feedback systems. *IEEE Trans. Automat. Contr.*, 30:240–247, 1985.

[FG] R. Ford and K. Glover. An application of coprime factor based anti-windup and bumpless transfer control to the spark ignition engine idle speed. In *Proc of Conference on Dec. and Contr.*

[FL98] U. Forsell and L. Ljung. Closed loop identification revisited. Technical report, Linköping University, 1998.

[Fle87] R. Fletcher. *Practical Methods of Optimisation.* John Wiley and Sons, 1987.

[GM89] K. Glover and D. McFarlane. Robust stabilisation of normalised coprime factor plant descriptions with $\mathcal{H}_\infty$-bounded uncertainty. *IEEE Trans. Automat. Contr.*, (34):821–830, 1989.

[GS90] T. T. Georgiou and M. C. Smith. Optimal robustness in the gap metric. *IEEE Trans. Automat. Contr.*, 35:673–687, 1990.

[Lju99] L. Ljung. *System Identification: Theory For The User.* Prentice Hall, 1999.

[Par92] J. R. Partington. Approximation of unstable infinite-dimensional systems using coprime factors. *Syst. and Contr. Lett.*, 16:89–96, 1992.

[PG99] G. Papageorgiou and K. Glover. $\mathcal{H}_\infty$ loopshaping: Why is it a sensible procedure for designing robust flight controllers? In *Proc. of AIAA conf. on Guidance, Navigation and Control*, 1999.

[vdHS95] P. M. J. van den Hof and R. J. P. Schrama. Identification and control - closed loop issues. *Automatica*, 31:1751–1770, 1995.

[Vid84] M. Vidyasagar. The graph metric for unstable plants and robustness estimates for feedback stability. *IEEE Trans. Automat. Contr.*, 29:403–418, 1984.

[Vid85] M. Vidyasagar. *Control Systems Synthesis: A Facorisation Approach.* MIT Press, 1985.

[Vin93a] G. Vinnicombe. Frequency domain uncertainty and the graph topology. *IEEE Trans. Automat. Contr.*, 38:1371–1383, 1993.

[Vin93b] G. Vinnicombe. *Measuring the robustness of feedback systems.* PhD thesis, University of Cambridge, 1993.

[Vin96] G. Vinnicombe. The robustness of feedback systems with bounded complexity controllers. *IEEE Trans. Automat. Contr.*, 41:795–803, 1996.

[Vin01] G. Vinnicombe. *Uncertainty and Feedback: $\mathcal{H}_\infty$ loop-shaping and the $\nu-$gap metric.* Imperial College Press, 2001.

[XFS01] L. Xie, E. Friedman, and U. Shaked. Robust $\mathcal{H}_\infty$ control of distributed delay systems with application to combustion control. *IEEE Trans Automat. Contr.*, 2001.

[ZDG96] K. Zhou, J.C. Doyle, and K. Glover. *Robust and Optimal Control*. Prentice Hall, 1996.